Proc. Natl. Acad. Sci. USA
Vol. 91, pp. 8224–8228, August 1994
Biochemistry

Electron microscopic studies of the interaction between a *Bacillus subtilis* α/β-type small, acid-soluble spore protein with DNA: Protein binding is cooperative, stiffens the DNA, and induces negative supercoiling

(electron microscopy/DNA binding protein/cyclization)

JACK GRIFFITH*, ALEXANDER MAKHOV*, LETICIA SANTIAGO-LARA†, AND PETER SETLOW†‡

*Lineberger Comprehensive Cancer Center, University of North Carolina at Chapel Hill, Chapel Hill, NC 27599-7295; and †Department of Biochemistry, University of Connecticut Health Center, Farmington, CT 06030-3305

Communicated by Nicholas R. Cozzarelli, April 28, 1994

ABSTRACT **DNA within spores of *Bacillus subtilis* is complexed with a group of α/β-type small acid-soluble spore proteins (α/β-type SASPs), which have almost identical primary sequences and DNA binding properties. Here electron microscopic and cyclization studies were carried out on α/β-type SASP–DNA complexes. When an α/β-type SASP was incubated with linear DNA, the protein bound cooperatively, forming a helical coating 6.6 ± 0.4 nm wide with a 2.9 ± 0.3 nm periodicity. α/β-Type SASP binding to an 890-bp DNA was weakest at an (A+T)-rich region that was highly bent, but binding eliminated the bending. α/β-Type SASP binding did not alter the rise per bp in DNA but greatly increased the DNA stiffness as measured by both electron microscopic and cyclization assays. Addition of α/β-type SASPs to negatively supertwisted DNA led to protein binding without significant alteration of the plectonemically interwound appearance of the DNA. Addition of α/β-type SASPs to relaxed or nicked circular DNA led to molecules that by electron microscopy appeared similar to supertwisted DNA. The introduction of negative supertwists in nicked circular DNA by α/β-type SASPs was confirmed by ligation of these molecules followed by topoisomer analyses using agarose gel electrophoresis.**

Work on the binding of α/β-type small, acid-soluble spore proteins (SASPs) from *Bacillus* and *Clostridium* species to DNA (1, 2) raised a number of structural questions that could be addressed by an electron microscopic (EM) study of α/β-type SASP DNA binding. Among these questions is whether the rise per bp of the DNA is altered upon binding of α/β-type SASP. Previous observations have suggested that the helical parameters of DNA may be altered by α/β-type SASP binding (3, 4). Thus it would be valuable to know if DNA is extended or shortened by α/β-type SASP binding. Second, previous studies suggested that the binding of α/β-type SASP to DNA is cooperative (1, 2). Direct visualization of α/β-type SASP–DNA interaction should verify this and determine whether DNA is stiffened, bent, or coiled upon protein binding. Finally, EM might discern how α/β-type SASPs induce negative supercoiling in DNA (1, 5). Previous work showed that incubation of relaxed covalently closed DNA with α/β-type SASP followed by treatment with topoisomerase I led to DNA with increased negative supercoiling (1). Binding of α/β-type SASP to DNA could induce negative supercoiling by two classical mechanisms: (*i*) by forming nucleosome-like particles about which the DNA would wind in a left-handed fashion and (*ii*) by partially unwinding circular DNA, leading to negative supercoiling following treatment with topoisomerase I and removal of the protein. Examples of supercoiling induced by the latter mechanism are the unwinding of DNA by intercalating drugs or the *Escherichia coli* RecA protein (6, 7). In these cases the DNA is extended 1.5-fold and unwound 12–13°/bp (reviewed in ref. 8). Another possible cause for the unwinding of circular DNA upon protein binding is the conversion of DNA from a B-like to an A-like helix, as A-DNA may have more base pairs per turn of the helix than B-DNA. This has been suggested to be the cause of the negative supercoiling induced by the binding of α/β-type SASP to covalently closed plasmids (1, 5).

MATERIALS AND METHODS

DNA and Proteins. The 890-bp DNA fragment containing a 223-bp (A+T)-rich insert from *Crithidia fasciculata* has been described (9). The 1325-bp blunt-ended fragment was purified from *Bal* I–*Hpa* I-cut M13mp7 double-stranded DNA on a 10% acrylamide gel. The 392-bp DNA used for negative staining was amplified by PCR from a pUC13-based plasmid carrying the adenovirus major late promoter. Plasmid pUC19 and pUR222 DNAs were isolated by standard methods. Singly nicked circular forms of these plasmids were generated as described by Greenfield *et al.* (10) and purified by banding in a CsCl gradient.

The α/β-type SASP SspC of *Bacillus subtilis* and SASP-β of *Clostridium bifermentans* were purified as described (1, 11).

Cyclization Assays. Protein and DNA were preincubated in 17 μl of 25 mM Tris acetate (pH 7.0) and 1 mM EDTA. The concentration of DNA fragment used was generally 60 nM in ends. The relatively weak interaction between α/β-type SASP and DNA (2) dictated this rather high DNA concentration (12, 13) to avoid using the high protein/DNA ratios required when low DNA concentrations are employed. After 1 hr at 30°C, the incubations were made 10 mM in $MgCl_2$ and 0.9 mM in ATP, and 1 unit of T4 DNA ligase was added to give a total volume of 20 μl. After 2 hr at room temperature, protein was removed and DNA was precipitated by addition of 60 μl of 1.25% SDS and 25 mM EDTA, 4 μl of 5 M NaCl, and 2 volumes of ethanol. The precipitated DNA was fractionated by electrophoresis on 0.8% agarose gels. The migration positions of various ligation products (as well as their identification as circular or linear molecules) were determined as described (12).

Topoisomer Analyses. Singly nicked, covalently closed plasmid pUC19 DNA (0.5 μg) purified by banding in CsCl

The publication costs of this article were defrayed in part by page charge payment. This article must therefore be hereby marked "*advertisement*" in accordance with 18 U.S.C. §1734 solely to indicate this fact.

Abbreviations: SASP, small, acid-soluble spore protein; EM, electron microscopy

‡To whom reprint requests should be addressed.

was incubated in 20 μl of 50 mM Tris, pH 7.6/10 mM $MgCl_2$/1 mM ATP/1 mM dithiothreitol with or without a saturating level of SspC (4 μg). After 30 min at room temperature, 1 unit of T4 DNA ligase was added, incubation was continued for 2 hr at room temperature, and the DNA was isolated as described above. Topoisomers were separated by electrophoresis in agarose gels containing chloroquine, and the number of negative supertwists [i.e., ΔLk (14)] induced by SspC binding was quantitated as described (1, 5).

Preparation of Samples for EM. Preparation of samples for rotary shadowcasting followed Griffith and Christiansen (15) beginning with 0.6% glutaraldehyde treatment for 5 min at room temperature, followed by chromatography over 2-ml columns of Bio-Gel A5M (equilibrated in 10 mM Tris, pH 7.5/0.1 mM EDTA) or direct dilution in this buffer to 0.5–1.0 μg of DNA per ml. The samples were mixed with a buffer containing 1 mM spermidine and 0.15 M NaCl, applied to freshly glow-charged carbon foils supported by 400-mesh copper grids for 30 s, and washed with water/ethanol solutions prior to air-drying and rotary shadowcasting with tungsten. Micrographs were taken using a Philips EM400TLG instrument. Length measurements were made by projecting images of molecules onto a Summagraphics digitizing tablet and tracing molecule contours using software developed in this laboratory. For negative staining, samples of DNA and SspC mixed at a mass ratio of 1:5 were incubated for 5 min at 30°C and stained without fixation using 2% uranyl acetate in water. Dimensions of the complexes were measured from the images using a charged coupled device camera and the National Institutes of Health image software and applying the edge detection criterion described by Steven *et al.* (16).

RESULTS

Visualization of the Binding of α/β-Type SASP to Linear DNA. To examine the binding of α/β-type SASP to linear DNA, SspC was diluted to 500 μg/ml in 20 mM Hepes buffer (pH 7.0) and mixed with DNA (1 μg/ml) in the same buffer at ratios from 1:1 to 10:1 (μg of protein/μg of DNA). Following incubation for 5 min at 37°C, samples were fixed and prepared for EM (*Materials and Methods*). At ratios of SspC:DNA below 5:1 tracts of protein-bound and protein-free DNA were observed, suggesting cooperative binding and stiffening of the DNA (Fig. 1*A*). The diameter of the filament was severalfold that of DNA (see below). At SspC:DNA ratios of 5:1 or greater, the DNA was fully covered. Shown in Fig. 1*B* are several DNA fragments fully covered with SspC following incubation at a 6:1 ratio. A frequent occurrence once the DNA was fully covered by α/β-type SASP was the formation of large side-by-side aggregates of the filaments (Fig. 1*C*), which sequestered more and more of the DNA, as the amount of protein increased.

Measurement of the length of the 890-bp DNA fragment without SspC gave values ranging from 0.256 to 0.283 μm (median, 0.274 μm; $n = 13$). When fully covered by SspC, the protein–DNA filament lengths ranged from 0.254 to 0.288 μm (median, 0.268 μm; $n = 71$). These values indicate that there is no significant change (≤5%) in the length of the DNA helix, and thus the apparent rise per bp, upon binding of α/β-type SASP.

Elimination of Sequence-Directed DNA Bending Upon α/β-Type SASP Binding. In the DNA fragment used above (9), nonbent DNA flanks both sides of a 223-bp highly bent segment from *C. fasciculata* containing 18 tracts of four to six adenines. At the center of this 223-bp segment is an 18-bp run that is 95% A+T (17). In the experiments above (SspC:DNA ratios of 6:1), roughly 30% of the molecules showed a small gap in the protein sheath (Fig. 2). The position of this gap measured 317 bp from the nearest DNA end: the center of the bent helix segment and (within measurement error) the site of the highly (A+T)-rich segment. For those molecules that were fully covered by SspC, no evidence of a bend could be seen. Thus, in agreement with earlier work, α/β-type SASP binding is weakest to (A+T)-rich segments (2), and further binding is not inhibited by sequence bends, but rather binding appears to remove sequence-dependent bends.

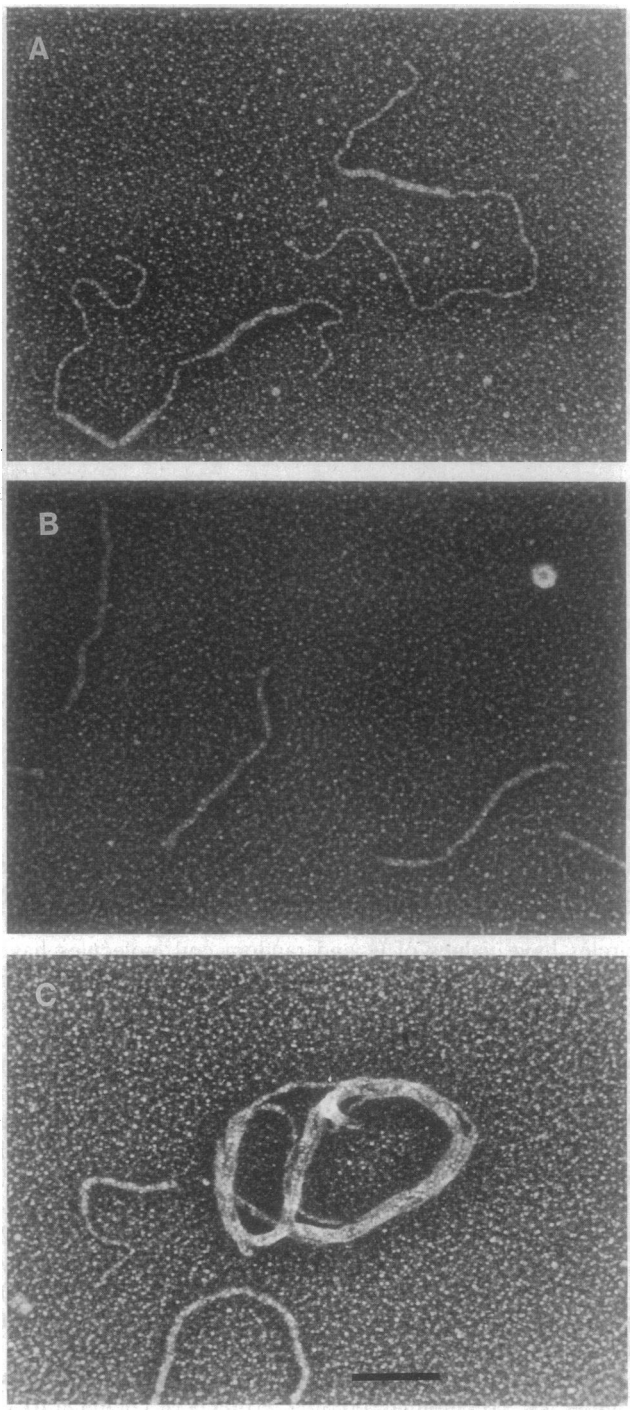

FIG. 1. Visualization of α/β-type SASP bound to linear DNA. SspC was incubated with linear *Eco*RI-cut pUC19 DNA (*A* and *C*) or the 890-bp DNA fragment (*B*) at ratios of 2:1 (*A*), 6:1 (*B*), or 10:1 (*C*) (μg of protein/μg of DNA) as described in the text, fixed, and prepared for EM, including adsorption to thin carbon supports, washing, drying, and rotary shadowcasting with tungsten. Images are shown in reverse contrast. (*A*) Cooperatively bound tracts of SspC on pUC19. (*B*) Fully complexed DNA. (*C*) Side-by-side aggregate of SspC-complexed pUC19 filaments. (Bar = 0.1 μm.)

EM Analysis of the Stiffening of DNA by α/β-Type SASP. To quantitate the stiffening of DNA by α/β-type SASP, the

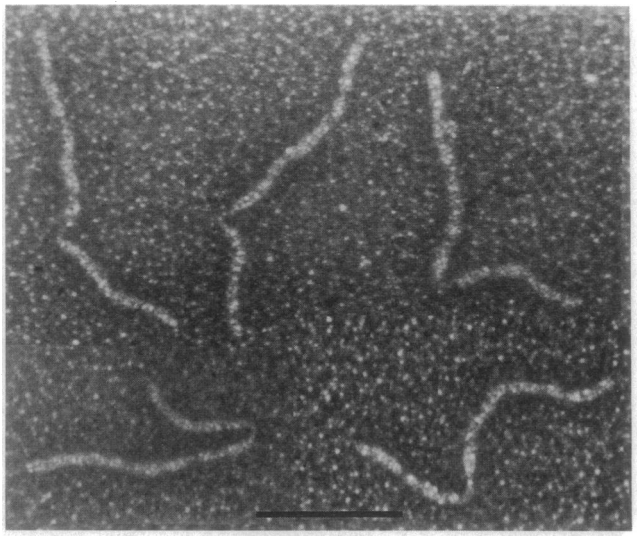

FIG. 2. Binding of α/β-type SASP to a DNA containing an (A+T)-rich bent helix segment. The 890-bp DNA used here contains a highly bent 223-bp segment from *C. fasciculata* (9) that lies 206 bp from one end of this DNA and 471 bp from the other. At the center of this 223-bp element is an 18-bp segment that is 95% A+T. Here this DNA was complexed with SspC at a 6:1 ratio, fixed, and prepared for EM as in Fig. 1. Molecules containing a protein-free gap in the bent region comprised roughly 30% of the population; a number of such examples are shown here. These gaps encompass only a small portion of the 223-bp bent segment that maps to the segment that is 95% A+T. (Bar = 0.1 μm.)

straight line distance (E–E) between the ends of a protein-free or protein-bound DNA was divided by its curvilinear length (L). Rod-like molecules have E–E/L values approaching 1.0, circles have values of 0, and random coil molecules have disperse values, most falling below 0.5 (18, 19). A 1325-bp DNA fragment lacking any sequence-dependent bends was used. The DNA (20 μg/ml) without or with SspC (100 μg/ml) was incubated for 30 min on ice in a buffer containing 20 mM Hepes (pH 7.0), 50 mM KCl, and 1 mM EDTA, fixed with 0.6% glutaraldehyde for 5 min, and prepared for EM. The average E–E/L value for the protein-free DNA was 0.386 and for the SspC–DNA filaments it was 0.722 (data not shown). In addition, while the protein-free DNA had a broad distribution of values with numerous ones (≈20%) at or below 0.2 and none above 0.85, the SspC–DNA filament values nearly all (>94%) lie at or above 0.5 and a significant fraction (56%) fall at or above 0.9, which is equivalent to a very straight molecule.

EM of Negatively Stained, Unfixed α/β-Type SASP–DNA Complexes. To eliminate possible artifacts of chemical fixation, negative staining of unfixed SspC–DNA complexes was carried out. This analysis also provided an accurate measurement of the parameters of SspC–DNA filaments. Images of the complexes (Fig. 3 *A–C*) revealed stiff DNA–protein filaments 6.6 ± 0.4 nm in width with a repeating substructure. Analysis of such images led to a model (Fig. 3*D*) in which the protein forms a helical array around the DNA helix and shifts the DNA into a form slightly different from the normal B-form structure. The period of the repeat along the filament measured 2.86 ± 0.26 nm, the width of the protein particles making up the repeat was 1.9 ± 0.2 nm, and the angle that the protein particles made along the filament with respect to the helix axis (along straight segments) was 54° ± 5°. These values are depicted in Fig. 3*D*. Measurement of the length of fully protein-covered filaments yielded a value of 134 ± 14 nm, equivalent to a separation of base pairs in the filament of 0.34 nm.

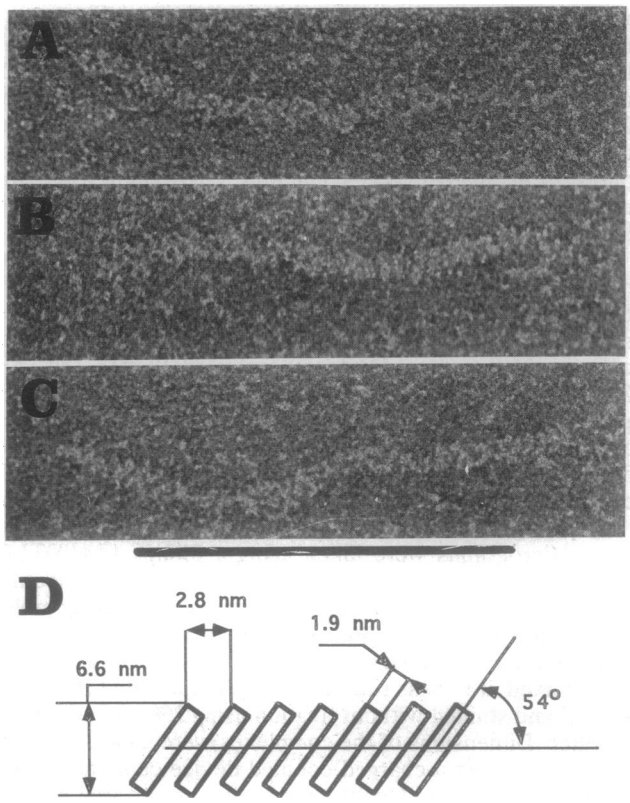

FIG. 3. Visualization of unfixed α/β-type SASP–DNA complexes by negative staining. (*A–C*) SspC was incubated in 20 mM Hepes (pH 7.0) with a nonbent 392-bp DNA at a 5:1 protein to DNA ratio, incubated for 5 min at 30°C, and directly applied to a glow-charged thin carbon foil without exposure to fixatives or spermidine. The sample was then stained with 2% uranyl acetate. A protein-free DNA segment can be seen in *A*. Bar equals 100 nm. (*D*) Model depicting the helical parameters of these filaments.

Effect of α/β-Type SASP on DNA Cyclization. To obtain further evidence for the stiffening of DNA by α/β-type SASP binding, we measured the effect of these proteins on cyclization of DNA fragments by DNA ligase. Treatment of a 2.7-kb fragment without SspC generated a large amount (20–30% of the total) of various circular forms, with the cyclized monomer predominating (Fig. 4, lane 1). However, addition of SspC resulted in a decrease in the yield of cyclized monomer

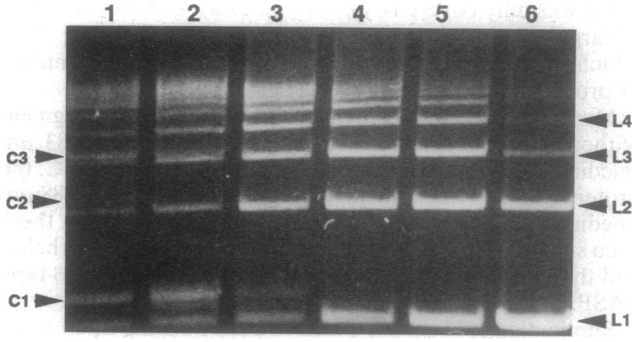

FIG. 4. Effect of α/β-type SASP on DNA cyclization by DNA ligase. Ligation reactions (20 μl) were carried out with 1 μg of *Pst* I-linearized pUC19 (2.7 kb) per tube and analyzed as described in the text. The amount of SspC added to the samples in the various lanes was none (lane 1), 2 μg (lane 2), 3 μg (lane 3), 4 μg (lane 4), 5 μg (lane 5), 10 μg (lane 6). The arrows labeled L1, L2, L3, and L4 denote the migration positions of linear monomer, dimer, trimer, and tetramer. The arrows labeled C1, C2, and C3 denote the migration positions of circular monomer, dimer, and trimer.

and an increase in linear dimers, trimers, etc. (Fig. 4, lanes 2–6). The SspC:DNA ratio above which no more (<3% of the total) circular monomer was generated was ≈4:1, which is the ratio at which DNA is saturated by α/β-type SspC (2). At this protein/DNA ratio there was still significant DNA ligation, as a large amount of linear products was formed (Fig. 4, lane 4). However, as the SspC/DNA ratio was further increased, there was significant inhibition of DNA ligation (Fig. 4, lane 6). Other experiments (data not shown) showed that binding of SspC to 194-, 310-, 480-, 625-, and 1300-bp DNA fragments abolished their cyclization, that cyclization of the 480-bp and 2.7-kb DNAs was abolished upon binding of another α/β-type SASP, SASP-β from *C. bifermentans*, and that an SspC variant, termed $SspC^{ala}$, that does not bind DNA (20) had no effect on ligation products. While SspC binding could inhibit DNA cyclization for a variety of reasons (for example, sequestration of DNA in complexes that cannot cyclize), this inhibition is certainly consistent with the EM analyses of fixed and unfixed samples which indicate that DNA is greatly stiffened by α/β-type SASP binding. However, it is possible that the results from the cyclization assays reflect both DNA stiffening as well as another effect of the binding of α/β-type SASP to DNA.

Visualization of the Binding of α/β-Type SASP to Circular DNAs. Negatively supertwisted pUR222 DNA (2.2 kb) (>95% supertwisted with an average of 10 or 11 supertwists per molecule as counted by EM) was mixed with SspC in 20 mM Hepes (pH 6.7), 50 mM KCl, and either 1 mM EDTA or 1, 5, or 10 mM $MgCl_2$. Incubation was for 30 min to 18 hr on ice followed by dilution of the sample to 1 μg of DNA per ml and preparation for EM. Under no combinations of incubation times or amounts of SspC or $MgCl_2$ were relaxed or mostly relaxed pUR222 circles observed above the 5% background in the protein-free DNA. Rather, the plectonemically interwound appearance of the protein-free DNA was retained. As increasing amounts of SspC were added, tracts of protein-coated DNA (arrows, Fig. 5*A*) were apparent, but the DNA retained an overall supertwisted appearance (a DNA molecule with little if any SspC bound is in Fig. 5*A*) and frequently appeared more twisted than the protein-free DNA. Upon extended incubation, or at higher protein/DNA ratios, aggregation of the DNA into very dense bodies and networks occurred.

Circular pUR222 DNA that was 98% singly nicked as determined by EM was also used as a substrate in parallel with reactions employing negatively supercoiled DNA. Here, with 5:1 protein/DNA ratios or short (1–5 min) incubations on ice, some of the DNA appeared as relatively open circles but with domains that appeared pinched off due to the local binding of the protein and its propensity to align the DNA strands side-by-side (Fig. 5*B*, arrows on molecules on left). However, many molecules appeared very similar to the negatively supercoiled pUR222 DNA circles coated with SspC (compare Fig. 5*B*, molecules on right, with Fig. 5*A*) and at protein/DNA ratios of 10:1, up to 50% of the nicked DNA circles had this appearance. At ratios of 20:1 an even larger fraction of the DNA was in this form, but this was difficult to quantitate. Further, although the strands appeared to wrap about each other, it was difficult to count the number of crossovers from the EMs. Nonetheless, when possible, such counts of molecules fully complexed by SspC yielded values of 8–10 crossovers (or nodes), a value approaching the number (10 or 11) in the supercoiled pUR222 DNA used. Use of covalently closed and topologically relaxed DNA gave results essentially identical to those obtained with the nicked circular DNA—i.e., generation of apparent supertwists upon SspC binding with approximately the same number of nodes per DNA molecule (data not shown).

Measurement of the generation of supertwists in nicked circular pUC19 DNA upon SspC binding by treating the SspC–DNA complex with DNA ligase followed by agarose gel electrophoretic analysis gave results similar to those obtained by EM. While ligation of nicked plasmid DNA in the absence of SspC generated covalently closed and relaxed DNA circles, the presence of saturating SspC levels during ligation resulted in covalently closed plasmid with an average value for ΔLk (14) of −16 (data not shown). This latter value is similar to that obtained by topoisomerase I treatment of relaxed covalently closed pUC19 DNA that is saturated with SspC (ref. 1; data not shown).

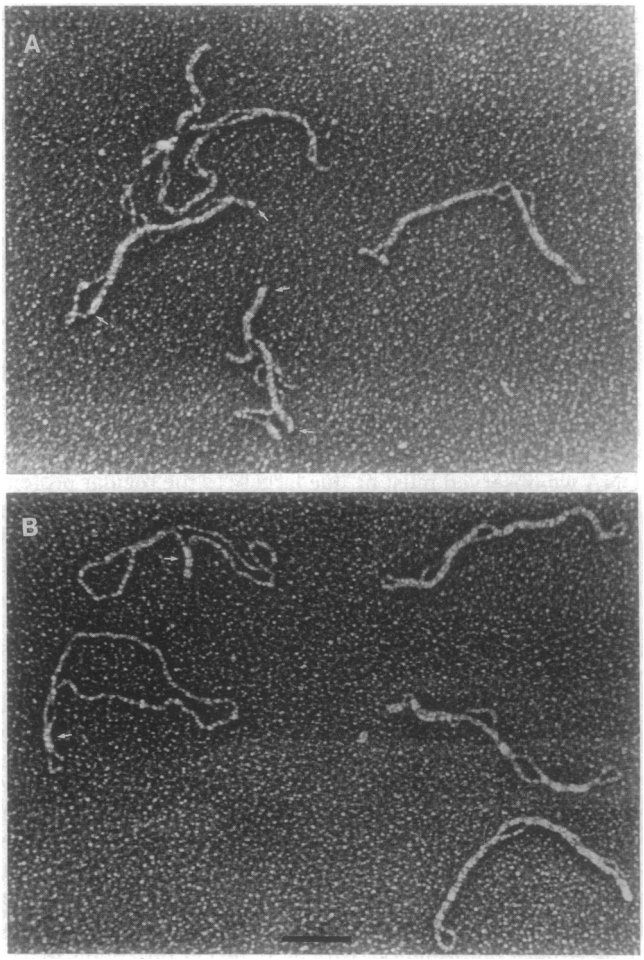

FIG. 5. Visualization of the binding of α/β-type SASP to circular DNA. (*A*) pUR222 DNA consisting of >95% supertwisted molecules was complexed with SspC as described in the text at an SspC/DNA ratio of 10:1. Following a 30-min incubation on ice, the samples were fixed and processed for EM (see Fig. 1 and text). Here tracts of SspC coverage along the plectonemically interwound DNA can be seen (arrows). The top-most molecule appears indistinguishable by EM from pUR222 DNA prepared in this manner without SspC. (*B*) SspC at a protein/DNA ratio of 5:1 was incubated with nicked circular pUR222 DNA consisting of >98% nicked circles in parallel with *A* above. Here a mixture of species was present in which (left) open circles with domains being pinched off by SspC binding (arrows) were observed together with (right) molecules that appeared typical of the interwound supertwisted DNA. The molecules on the left were added to create the photographic montage (*Materials and Methods*). (Bar = 0.1 μm.)

DISCUSSION

The findings described here confirm several conclusions drawn from previous studies, as both the cooperative binding of α/β-type SASPs to DNA as well as their relatively weak binding to (A+T)-rich regions have been shown by other techniques (1, 2, 4). Previous spectroscopic analysis indi-

cated that α/β-type SASP binding changes DNA from a B-like to an A-like helix (3). Here EM measurements showed that the rise per bp in DNA is unaltered by α/β-type SASP binding. Thus the A-like DNA structure detected spectroscopically cannot be similar to a "classic" A-DNA in which the rise per bp is decreased $\approx$25% relative to that in B-DNA. However, the rise per bp of A-like DNAs can vary significantly, with some A-like helices having values for rise per bp essentially identical to those of B-like DNAs (21, 22). Clearly, further structural analyses of the structure of α/β-type SASP–DNA complexes are warranted.

The observation that α/β-type SASP binding stiffens DNA has, to our knowledge, not been reported previously, and the inhibition of cyclization for DNAs up to 2.7-kb suggests that α/β-type SASP binding must increase DNA persistence length at least 20-fold (23). Although A-like DNA is stiffer than B-form DNA by roughly 3-fold (24), the stiffening of DNA we observed must be due largely to the regular protein helix formed around the DNA. One interesting feature of the observations that α/β-type SASP binding stiffens DNA and that binding is relatively weak to (A+T)-rich segments is that during the folding of the *B. subtilis* chromosome in a spore, were there (A+T)-rich segments spaced at uniform distances along the DNA, then these segments could serve as swivels that would aid in folding the DNA back and forth on itself.

Previous work (1) used topoisomerase treatment and gel electrophoresis to show that α/β-type SASP binding to relaxed circular DNA induces negative supertwisting in DNA. Here we excluded the possibility that this arises by formation of nucleosome-like particles. Instead, α/β-type SASP binding together with topoisomerase action must have placed the relaxed DNA circles in a conformation that created negative supercoiling. It was suggested that the negative supercoiling resulted from an alteration of the DNA to an A-like conformation (with more bp per turn of the helix; ref. 1), and this was supported by the spectroscopic data (3). Now, based on the data presented here, we must further propose that α/β-type SASP binding to circular DNA pinches off topological domains. Given the propensity of α/β-type SASP to bring two DNA helices together in side-by-side association, this does not seem unreasonable.

In an alternative, and more novel, model whereby α/β-type SASPs induce DNA supercoiling, the protein has no effect on the bp per turn of the DNA helix. Rather, protein binding promotes side-by-side association of two DNA helices and also gently winds the helices around one another, generating an overall twisting that has the same handedness as the DNA helix itself. This model is consistent with all of the data, in particular with the agreement between the values for ΔLk/kb (-6) induced by α/β-type SASP binding to either nicked circular DNA (determined following ligation in this work) or relaxed covalently closed DNA [determined following topoisomerase treatment (1)]. The value for nodes per kb determined by EM on nicked circular DNA complexes with SspC ($\approx$4.1 per kb) is below the value for ΔLk/kb. However, there are theoretical reasons (14) why ΔLk/kb should have a larger absolute value than nodes per kb, and EM measurements undoubtedly underestimate nodes. One serious complication of this model is that it is difficult to imagine how a relatively nonspecific DNA binding protein could stabilize only negative nodes in DNA. Consequently, this explanation seems less likely than the one given above.

Some combination of the propensities of α/β-type SASP to stabilize nodes in DNA and to unwind DNA may provide separate explanations for the different EM experiments. Thus binding of α/β-type SASP to relaxed circular DNA may partially unwind the DNA, initiating a gentle plectonemic coiling of the strands about each other, with this coiling stabilized and possibly magnified by the propensity of these proteins to pinch off topological domains. However, when α/β-type SASP is added to negatively supercoiled DNA, the stabilization of nodes by protein binding may inhibit the protein-induced unwinding from generating topologically relaxed DNAs as seen in the EM.

We thank Carl Bortner for carrying out initial EM experiments, Waltraut Waterman for preliminary cyclization experiments, and Kartik Natarajan for agarose gel electrophoretic analyses. This work was supported in part by grants to J.G. from the American Cancer Society (NP 583) and the National Institutes of Health (GM31819) and to P.S. from the National Institutes of Health (GM19698).

1. Nicholson, W. L., Setlow, B. & Setlow, P. (1990) *J. Bacteriol.* **172,** 6900–6906.
2. Setlow, B., Sun, D. & Setlow, P. (1992) *J. Bacteriol.* **174,** 2312–2322.
3. Mohr, S. C., Sokolov, N. V. H. A., He, C. & Setlow, P. (1991) *Proc. Natl. Acad. Sci. USA* **88,** 77–81.
4. Nicholson, W. L., Setlow, B. & Setlow, P. (1991) *Proc. Natl. Acad. Sci. USA* **88,** 8288–8292.
5. Nicholson, W. L. & Setlow, P. (1990) *J. Bacteriol.* **172,** 7–14.
6. Chrysogelos, S., Register, J. C., III, & Griffith, J. (1983) *J. Biol. Chem.* **258,** 12624–12631.
7. Stasiak, A., DuCapua, E. & Koller, T. H. (1981) *J. Mol. Biol.* **151,** 557–564.
8. Thresher, R. & Griffith, J. D. (1990) *Proc. Natl. Acad. Sci. USA* **87,** 5056–5060.
9. Laundon, C. H. & Griffith, J. D. (1987) *Biochemistry* **26,** 3759–3762.
10. Greenfield, L., Simpson, L. & Kaplan, D. (1975) *Biochim. Biophys. Acta* **407,** 365–375.
11. Cabrera-Martinez, R. M., Setlow, B., Waites, W. M. & Setlow, P. (1989) *FEMS Microbiol. Lett.* **61,** 139–144.
12. Hodges-Garcia, Y., Hagerman, P. J. & Pettijohn, D. E. (1989) *J. Biol. Chem.* **264,** 14621–14623.
13. Thomas, T. J. & Bloomfield, V. A. (1983) *Nucleic Acids Res.* **11,** 1919–1930.
14. Cozzarelli, N. R., Boles, T. C. & White, J. H. (1990) in *DNA Topology and Its Biological Effects*, eds. Cozzarelli, N. R. & Wang, J. C. (Cold Spring Harbor Lab. Press, Plainview, NY), pp. 139–184.
15. Griffith, J. D. & Christiansen, G. (1978) *Annu. Rev. Biophys. Bioeng.* **7,** 19–35.
16. Steven, A. C., Trus, B. L., Maizel, J. V., Unser, M., Parry, D. A. D., Wall, J. S., Hainford, J. F. & Studier, F. (1988) *J. Mol. Biol.* **200,** 351–365.
17. Wang, Y.-H., Howard, M. & Griffith, J. D. (1991) *Biochemistry* **30,** 5443–5449.
18. Joanicot, M. & Revet, R. (1987) *Biopolymers* **26,** 315–326.
19. Revet, B., Malinge, J. M., Delain, E., Le Bret, M. & Leng, M. (1984) *Nucleic Acids Res.* **12,** 8349–8362.
20. Tovar-Rojo, F. & Setlow, P. (1991) *J. Bacteriol.* **173,** 4827–4835.
21. Jain, S. & Sundaralingam, M. (1989) *J. Biol. Chem.* **264,** 12780–12784.
22. Shakked, Z., Guerstein-Guzikevich, G., Eisenstein, M., Frolow, F. & Rabinovich, D. (1989) *Nature (London)* **342,** 456–460.
23. Shore, D., Langowski, J. & Baldwin, R. L. (1981) *Proc. Natl. Acad. Sci. USA* **78,** 4833–4837.
24. Charney, E., Chen, H.-H. & Rau, D. C. (1991) *J. Biomol. Struct. Dyn.* **9,** 353–362.